Inorganica Chimica Acta 509 (2020) 119666

Contents lists available at ScienceDirect

Inorganica Chimica Acta

journal homepage: www.elsevier.com/locate/ica

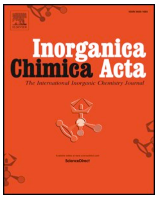

Research paper

Light-driven coordination anions-directed regulation of chromism in three metal complexes assembled by cyano-equipped dithienylethene ligand

Jing Han[a,c,*], Qing Li[a], Zhong Yu[b,*], Chun-yan Quan[a], Xiang Liu[a], Jia-cai Han[a]

[a] Department of Material Physics and Chemistry, Xi'an University of Technology, Xi'an, Shaanxi 710048, China
[b] Department of Chemistry, Xi'an University of Technology, Xi'an, Shaanxi 710048, China
[c] Department of Chemistry, University of California, Riverside, CA 92521, USA

ARTICLE INFO

Keywords:
Dithienylethene
Photochromism
Metal complexes
Anion effect
Crystal engineering

ABSTRACT

Three coordination compounds were self-assembled successfully with Ag(I) ions and photo-responsive ligands featuring a cyano-equipped dithienylethene unit. Anions with different coordinating abilities were selected to construct distinct topologies, which are evidenced by X-ray crystallographic analysis. CF_3COO^- and $CF_3SO_3^-$ are involved into coordination in **1** and **3**, respectively, whereas in **2** BF_4^- present merel y as ionic guests counterbalancing the framework charge. Anions also show their subtle effects on coordinated atoms, interactions, and ligand configurations. The quite different structures of **1–3** indicate an interesting anion-directed structural self-assembly.

Followed examinations on photochromism illustrated that the reversible photo-isomerizations of three complexes are all retained after complexzation with Ag(I) center. Various degrees of bathochromic shifts in absorptions were observed as compared with that of the metal-free ligand. Therefore, the photo-switching of these compounds could be modulated conveniently and finely by varying simply the coordination anions and then triggering by light irradiation. The discussions of structure-properties relationship concluded that anions exert their effects on coordination structure through adjusting the configurations of ligands in complexes. Strong coordinating anions facilitate a pronounced conformational change of ligand whereas un-coordinating anion leads to smaller variation. The distinct structural changes of ligand result finally the different perturbation of photochromic behavior.

1. Introductions

Dithienylethene (DTE) architectures responding to external input of light have stood out as excellent candidates for future applications as diverse as high-density information storage, switching devices and actuators owing to their reversible electronic as well as geometrical structure changes induced by chemical bond rearrangement during the photo-transformation between a non-conjugated open-form and a π-conjugated closed-form by alternate irradiation with UV and visible light [1–3]. For practical applications, improving their photophysical and photochemical properties has been especially concerned by optimizing the substitutes on the thienyl rings [4–6], addition of metal ions [7–10] and doping with composites [11–13]. Among these approaches, addressing metal centers to form hybrid materials through coordination with organic photo-responsive ligand could allow the combination of the advantages of both inorganic and photochromic organic species at the molecular level. Because metal complex plays the role of a photosensitizer in reversibly regulating the lifetime of the metal-ligand's excited state [14], incorporating dithienylethene into a complex system not only offers rich properties but also enables the regulation of the photo-switching performance, such as interesting spin-crossover [15–18], improved luminescence [19–22], NLO response [23,24] and porosity etc. [9,25,26], as demonstrated by several groups to date.

However, the existing explorations have mainly concentrated on the effect of metal ions [7–10], the contribution of coordination anions on photochromic behavior in solid state, from the crystal engineering point, has never been investigated systemically for dithienylethene species [27]. And anions were especially found to produce dramatic effects on the extended structure of the networks amongst those secondary driving forces, namely, pH value [28], temperature [29], reagent concentration [30] and solvent media [31]. We have previously synthesized a series of metal complexes with dithienylethene by designing dithienylethene ligands attached with various binding groups, including pyridine [32,33], carboxyl acid [34,35] and cyanophenyl [36]. Our results showed some successful examples of enhanced photo-switching in solid state after metal complexation, such as improved photo-stimulus [37] and suppressed side photoreaction [27] with only a few exceptions [38]. Our recent work indicated BF_4^-, a un-coordinating anion, is favorable for the

---

* Corresponding authors at: No. 5 South Jinhua Road, Xi'an, Shaanxi 710048, China.
E-mail addresses: hanj@xaut.edu.cn (J. Han), yuzhong@xaut.edu.cn (Z. Yu).

https://doi.org/10.1016/j.ica.2020.119666
Received 4 December 2019; Received in revised form 10 April 2020; Accepted 10 April 2020

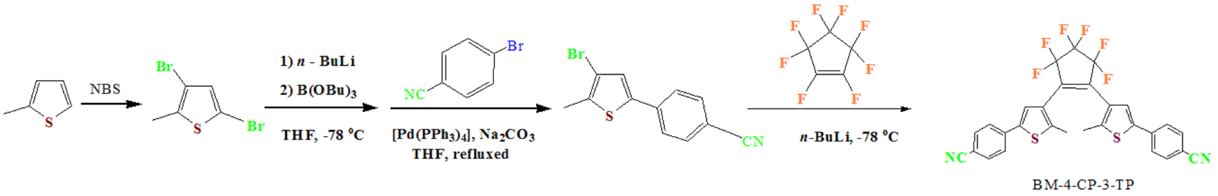

Scheme 1. Synthesis of BM-4-CP-3-TP.

effective photo-isomerization when it's self-assembled with *cis*-dbe into a coordination framework [27].

As an extension of our research interests and in order to further understand the exact role of anions in the modulations of photochromism, herein three Ag(I) salts with anions featuring distinct coordination affinities, i.e. CF_3COO^-, BF_4^- and $CF_3SO_3^-$, were selected judiciously to assemble with a photo-active dithienylethene ligand equipped with cyano groups. The ligand (1,2-bis-[2′-methyl-5′-(4″-cyanophenyl)-3′-thienyl] perfluorocyolopentene, hereafter referred as BM-4-CP-3-TP) was originally structural characterized by liu [39] and it shows effective photochromism in solution and film [40]. In this paper, three new complexes based on the ligand were isolated and structurally characterized by X-ray crystallography. And the relationships between crystal structures and solid state photo-switching were investigated further from the anions aspect.

2. Experimental

2.1. Material and methods

Unless otherwise indicated, all starting materials were obtained from commercial suppliers and without further purification prior to use. Infrared spectra were recorded as KBr disk on JASCO FT-IR 8000 spectrometers. Absorption spectra in solid state were measured by diffuse reflection using the Kubelka-Munk method on a SHIMADZU UV-3600 spectrometer, and barium sulfate was used as a reference. Absorption spectra in solutions were measured using a Hitachi U-3900 spectrometer. Solvent were used as purchased and not degassed. The concentration of solution is *ca.* 1×10^{-6} mol/L. PMMA film was prepared by solubilizing ultrasonically 10 mg complex and 100 mg PMMA in chloroform (1 mL), then spin-coating the homogeneous solution on a glass substrate (20 mm × 20 mm × 1 mm) with a spin rotation speed of 1500 rpm. Photo-irradiation was carried out using a 100 W Xe lamp in atmosphere, and light with appropriate wavelength was isolated by passing the light through andover filter (254 FS25) and RANYAN cut-off filter (BP 550–10 K). ^{1}HNMR spectra were measured on a Varian INOVA NMR spectrometer in $CDCl_3$ solution at room temperature (with Tetramethylsilane as internal reference).

2.2. X-ray data collection and structure solutions and refinements

Diffraction data for BM-4-CP-3-TP and complexes **1**–**3** were collected on BRUKER APEX-II CCD with graphite monochromated Mo-Kα radiation (λ = 0.71073 Å). The intensity data were collected at 296 K for all crystals, using the multi scan technique. The linear absorption coefficient μ for Mo-Kα radiation is 0.240, 1.043, 0.786 and 1.312 mm^{-1} for BM-4-CP-3-TP and complexes **1**–**3**, respectively. The structures were solved by direct methods followed by subsequent Fourier calculations. The non-hydrogen atoms were refined anisotropically. The final cycle of the full-matrix least squares refinement was based on 1095, 5759, 1942 and 2220 reflections for four crystals, respectively, converged with the unweighted and weighted agreement factors of $R = \Sigma||Fo|-|Fc||/\Sigma|Fo|$ and $Rw=(\Sigma w(Fo^2-Fc^2)^2/\Sigma w(Fo^2)^2)^{1/2}$. The atomic scattering factors and anomalous dispersion terms were taken from the International Tables for X-ray Crystallography, Vol. IV [41]. All calculations were performed using SHELXS-97 or SHELXS-2018/3 crystallographic software package [42,43].

2.3. Syntheses

1,2-bis-[2′-methyl-5′-(4″-cyanophenyl)-3′-thienyl] perfluorocyolopentene (BM-4-CP-3-TP). BM-4-CP-3-TP was prepared using modified literature method [39] (Scheme 1). *Anal.* IR (KBr pellet): 2360 (m), 2218 (m), 1595 (m), 1261 (m), 1101 (s), 983 (s), 823 (s), 743 (m). ^{1}HNMR ($CDCl_3$, 400 MHz, δ / ppm), 7.68 (d, 4H, *J* = 8.5 Hz, cyanophenyl H), 7.63 (d, 4H, *J* = 8.6 Hz, cyanophenyl H), 7.40 (s, 2H, thienyl H), 2.00 (s, 6H, methyl). Its single crystal was obtained by recrystallization from THF solution at room temperature and it's different from that of the previous compound [39].

$\{[Ag_2(BM\text{-}4\text{-}CP\text{-}3\text{-}TP)(CF_3COO)_2)]\cdot(C_6H_6)_2\}_n$ (1). Complex **1** was prepared by mixing of $AgCF_3COO$ (0.0162 g, 73 μmol) and **L** (0.0183 g, 32 μmol) in 2 mL benzene. After stirring for 30 min, the resultant solution was introduced into a 9 mm diameter glass tube and layered with *n*-pentane (2 mL) as a diffusion solvent. After standing at room temperature for one week, colorless crystals of **1** suitable for single crystal X-ray analysis were obtained. Yield: 38.32%. *Anal.* Calcd. for $C_{45}H_{28}Ag_2F_{12}N_2O_4S_2$ C, 46.25; N, 2.39; H, 2.42; S, 5.49; Found: C, 45.87; N, 2.84; H, 2.14; S, 5.84%. IR (KBr pellet): 2223 (m), 1680 (s), 1434 (m), 1267 (m), 1132 (w), 1106 (w), 830 (w), 806 (w), 743(w). ^{1}HNMR ($CDCl_3$, 400 MHz, δ/ppm), 7.68 (d, 4H, *J* = 8.2 Hz, cyanophenyl), 7.64 (d, 4H, *J* = 8.2 Hz, cyanophenyl), 7.40 (s, 2H, thienyl H) 7.37 (s, 6H, benzene), 1.99 (s, 6H, methyl).

Complex 1a. The benzene-eliminated **1a** was obtained by heating **1** for 1 h at 190 °C. ^{1}H NMR ($CDCl_3$, 400 MHz, δ/ppm): 7.68 (d, 4H, *J* = 8.0 Hz, cyanophenyl), 7.63 (d, 4H, *J* = 7.8 Hz, cyanophenyl), 7.40 (s, 2H, thienyl H), 1.99 (s, 6H, methyl).

Complex 1b. 1b was prepared by exposing **1a** to benzene vapor for 24 h at 50 °C, filtrated and dried. ^{1}H NMR ($CDCl_3$, 400 MHz, δ/ppm), 7.69 (d, 4H, *J* = 8.0 Hz, cyanophenyl), 7.64 (d, 4H, *J* = 8.0 Hz, cyanophenyl), 7.40 (s, 2H, thienyl H), 7.37(s, 6H, benzene), 1.99 (s, 6H, methyl).

Complex 1c. 1c was prepared by exposing **1a** to toluene vapor for 24 h at 50 °C, filtrated and dried. ^{1}H NMR ($CDCl_3$, 400 MHz, δ/ppm), 7.68 (d, 4H, *J* = 8.5 Hz, cyanophenyl), 7.63 (d, 4H, *J* = 8.5 Hz, cyanophenyl), 7.40 (s, 2H, thienyl H), 1.99 (s, 6H, methyl).

$\{[Ag(BM\text{-}4\text{-}CP\text{-}3\text{-}TP)]BF_4\cdot(THF)\}_n$ (2). To a benzene solution (15 mL) of **L** (0.057 g, 0.1 mmol) was added $AgBF_4$(0.019 g, 0.1 mmol). The resultant solution was stirred for 30 min and the resulted precipitate were dissolved in THF followed by filling in a long and narrow tube for slow evaporation. Colorless crystals were obtained after standing at room temperature for 1 week. Yield: 54%. *Anal.* Calcd. $C_{33}H_{24}AgBF_{10}N_2OS_2$ C, 47.33; N, 3.35; H, 2.89; S, 7.66; Found: C, 47.07; N, 3.65; H, 2.54; S, 7.86%. IR (KBr pellet): 2232 (m), 1600 (m), 1340 (m), 1274 (s), 1086 (w), 987 (w), 832 (w), 744 (w).

$\{[Ag_2(BM\text{-}4\text{-}CP\text{-}3\text{-}TP)(CF_3SO_3)_2(H_2O)_2]\}_n$ (3). Colorless crystals of **3** were grown similarly to those of **1** using ligand (0.057 g, 0.1 mmol) and $AgCF_3SO_3$ (0.026 g, 0.1 mmol). Yield: 45% (based on Ag). *Anal.* Calcd. $C_{31}H_{20}Ag_2F_{12}N_2O_8S_4$ C, 33.23; N, 2.50; H, 1.80; S, 11.45; Found: C, 33.57; N, 2.35; H, 1.94; S, 11.33%. IR (KBr pellet) 2231 (m), 1267 (s), 1175 (m), 1107 (w), 1037 (w), 831 (w), 646 (w).

3. Results and discussions

3.1. Infrared spectra analysis

The FT-IR spectra of complexes **1**–**3** are illustrated in Figs. S1–S3 to prove the formation of these complexes. The typical $C\equiv N$ stretching vibration peaks of cyanophenyl are found at 2221 cm^{-1} in ligand, and appeared at 2223 cm^{-1}, 2232 cm^{-1}, and 2231 cm^{-1} in complexes **1**–**3**, respectively. The red-shifts of $C\equiv N$ stretches are attributed to the π-back donation effect of cyano group [44,45], the s-donation as well as the electrostatic interaction [46–48]. The different shifts of the $C\equiv N$ frequency in **1** (+2 cm^{-1}) and **2**–**3** (+11 cm^{-1}) relative to the corresponding band in the free ligand may be ascribed to the subtle electrostatic interaction originating from their different structures. In addition, the characteristic νs(C-F) peak of perfluorocyclopentene in ligand at 1266 cm^{-1} are present at 1267 cm^{-1}, 1274 cm^{-1} and 1267 cm^{-1} in complexes **1**–**3**, respectively. These observations indicate that BM-4-CP-3-TP is included into all three complexes.

On the other hand, in the spectrum of **1**, the νs(C—O) peaks around 1680 cm^{-1} and 1434 cm^{-1} (1687 cm^{-1} and 1430 cm^{-1} for $AgCF_3COO$) as well as the νs(C-F) peak of 1132 cm^{-1} (1140 cm^{-1} for $AgCF_3COO$) indicate the presence of CF_3COO^-. Similarly, the typical peak of νs(B-F) of 1073 cm^{-1} appeared at 1056 cm^{-1} in the spectrum of **2**, suggesting the incorporation of BF_4^- into complex **2**. The stretching vibrations of $CF_3SO_3^-$, i.e. 1175 cm^{-1}, 1037 cm^{-1} and 646 cm^{-1}, are witnessed in the spectrum of **3**, demonstrating the existence of $CF_3SO_3^-$. These findings indicate that the respective anions are included in the frameworks of the three complexes.

3.2. Structural characterizations

The crystal structures of BM-4-CP-3-TP and complexes **1**–**3** are determined by X-ray single crystal diffractions. Details of the X-ray data are summarized in Table 1. Selected bond lengths and bond angles are given in Table S1.

3.2.1. Crystal structure of BM-4-CP-3-TP

For BM-4-CP-3-TP, it was firstly prepared in 2008 and its single crystals were crystallized from hexane [39]. In the present study, crystallization from THF led to the isolation of a new solvated form, which is different from the reported structure.

Fig. 1(a) depicts the crystal structure of BM-4-CP-3-TP·THF determined by X-ray crystallographic analysis. The THF molecules, using as crystallization solvent, are contained in the crystals and are disordered. The two thienyl rings are fixed in a photo-reactive anti-parallel conformation with the dihedral angel of 58.86° between two thienyl rings. The distance between reactive carbon atoms, C11 and C11A, is 3.65 Å. This anti-parallel conformation and a C···C distance less than 4.2 Å are mandatory for observing the photo-isomerization of the diarylethene unit in solid state. The cyanophenyl and thienyl rings are almost coplanar with the dihedral angel of 6.75° whereas in the reference crystals the dihedral angel is 22.43° [39]. This characteristic facilitates efficient electronic delocalization between the photoactive and the cyanophenyl moieties.

There are extensive intermolecular and intramolecular H contacts exist between two adjacent ligand molecules in BM-4-CP-3-TP·THF and two neighboring pairs of molecules are further interact with H bonds (Fig. 1(b) and (c)) which lead to a comparable closer packing than the referenced ligand where no H bonds present between two neighboring pairs of molecules (Fig. S4). The detailed bond distances and angels of both compounds are listed in Tables S2 and S3. The different packing modes of BM-4-CP-3-TP·THF and the referenced compound may be responsible for their different densities. The closer packing of BM-4-CP-3-TP·THF results in a smaller density of 1.394 g cm^{-3} (1.526 g cm^{-3} for referenced work).

In BM-4-CP-3-TP·THF, the dihedral angle between the mean planes of cyclopentene ring and the two thiophene rings is 51.26°. The mean torsion angle between thiophene and hexafluorocyclopentene rings (C13-C13A-C10A-C9A) is 128.71°. In the referenced structure, the mean torsion angle between thiophene and cyclopentene rings is −149.804°. The torsion angle between thiophene and hexafluorocyclopentene rings of BM-4-CP-3-TP·THF is significantly smaller than that of referenced structure, whereas the reactive distance of BM-4-CP-3-TP·THF (3.65 Å) is longer than that of referenced structure (3.60 Å).

3.2.2. Crystal structure of complex 1

Complex **1** is revealed as a 2D layer constructed by bridging ligand and 1D $AgCF_3COO$ chain. Benzene acts as guest intercalating between the adjacent layers. In one unit, there are two crystallographically independent Ag(I) centers with different coordination environments. Ag1 is four-coordinated to three O atoms from three CF_3COO^- anions (Ag1-O = 2.279(5)-2.477(7) Å) and one N atom from ligand (Ag1-N2C = 2.297(6) Å), showing a distorted tetrahedral structure. The structural distortion parameter τ_4 is 0.718 indicating of complex **1** a distorted trigonal pyramid (0.85 for prefect trigonal pyramid). The bottom plane of the trigonal pyramid is comprised of O1, O4 and N2C atoms with silver center lies out of the plane by the distance of 0.2033 Å. Ag2 is however surrounded by one O atom from CF_3COO^- anion and one N atom from ligand with N1-Ag2-O2 angle of 150.4(2)°, displaying a linear arrangement (Fig. 2(a)).

Two Ag1 ions are linked by two anions to form a four-membered ring. The neighboring Ag1 and Ag2 are bridged via one anion through two monodentated O atoms. The above arrangement leads to a Ag_4 cluster. These Ag_4 clusters are further interconnected each other by Ag···O interactions to generate a 1D chain along *b*-direction (Ag2-O2B = 2.6592(52) Å). Ag1···Ag2 distance is 3.1004 (9) Å, which is longer than the Ag-Ag separation in silver metal (2.89 Å) but shorter than twice the van der Waals radius of silver ions (3.44 Å), indicating weak Ag···Ag interaction [49]. From the perspective of anion, CF_3COO^-

Table 1
Crystal data of BM-4-CP-3-TP·THF and three complexes.

Compound	**BM-4-CP-3-TP·THF**	**1**	**2**	**3**
Formula	$C_{33}H_{24}F_6N_2OS_2$	$C_{45}H_{28}Ag_2F_{12}N_2O_4S_2$	$C_{33}H_{24}AgBF_{10}N_2OS_2$	$C_{31}H_{20}Ag_2F_{12}N_2O_8S_4$
Formula weight	642.66	1168.54	837.34	1120.47
Temperature/K	296(2)	296(2)	296(2)	296(2)
Crystal system, group	Monoclinic, C2/c	Triclinic, P-1	Monoclinic, P2(1)/c	Monoclinic, Cc
a/Å	20.26(2)	10.923(2)	13.923(9)	38.457(18)
b/Å	13.972(15)	11.512(2)	12.083(8)	9.260(4)
c/Å	10.816(13)	20.311(4)	21.164(13)	11.343(5)
α/(deg.)	90	74.918(3)	90	90
β/(deg.)	90.432	84.284(3)	103.077(13)	102.569(9)
γ/(deg.)	90	67.800(3)	90	90
Z, Dc (g/m^3)	4,1.394	2,1.700	4,1.604	4,1.888
μ (mm^{-1})	0.240	1.043	0.786	1.312
Reflections	2697/1095	9034/5759	6165/1942	3444/2220
Gof-fit on F^2	1.036	1.010	0.901	1.048
R_{all}/R_{get}	0.2109/0.1056	0.1019/0.0667	0.2771/0.0905	0.1368/0.0996
$wR2_{all}/wR2_{get}$	0.2962/0.2381	0.2345/0.1961	0.2948/0.1936	0.2652/0.2444

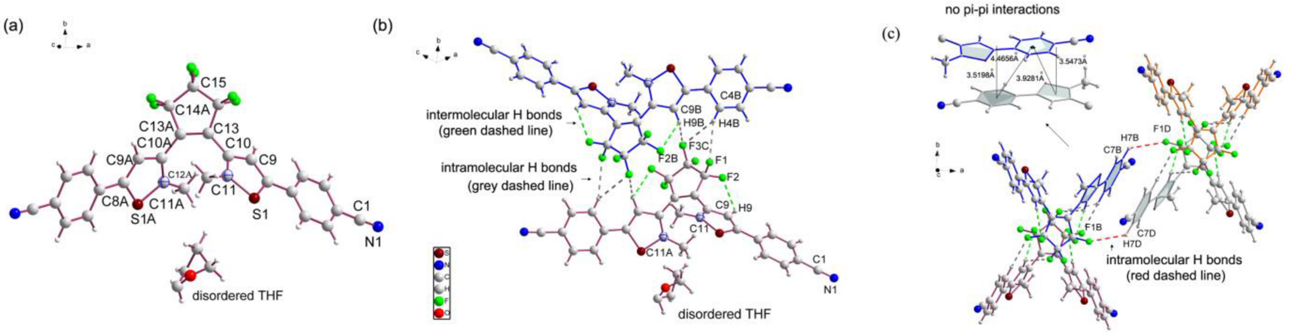

Fig. 1. Crystal structure of BM-4-CP-3-TP·THF (a) and its packing structures showing (b) H bonds and (c) interactions between molecules.

in **1** exhibits two kinds of coordination modes, i.e. μ_2-η^1:η^1-bridging mode and μ_2-η^2-bridging mode to join Ag centers, respectively.

In complex **1** the ligand acts as a bis-monodentate bridging linker through N atoms to spread the above mentioned 1D chain to a 2D layer. Benzene is intercalated within neighboring layers as guest. The nearest distance between Ag and benzene is 2.7767 Å, which is longer than the longest length of Ag-C coordination bond in published literatures (2.69 Å) indicating a cation-π interactions between the benzene and 2D layer [50]. Thus, in addition to filling the void spaces in the framework of **1**, the presence of guest benzenes can also contribute to the packing of **1** and enhance its stability.

For ligand, the two thienyl rings adopt anti-parallel fashions with dihedral angel of 61.23°. The two C atoms that are about to bind upon photo-cyclization (C15 and C25) keep 3.59 Å apart. The mean torsion angles between thiophene and hexafluorocyclopentene rings (C(17)-C(21)-C(22)-C(23) and C(21)-C(17)-C(14)-C(13)) are −134.1° and −129.13°, respectively. The cyanophenyl and thienyl rings are almost coplanar in free ligand, whereas this dihedral angel increase greatly from 6.75° to 40.07° after incorporation of Ag(I) ions. The bond length of C≡N in complex **1** (1.141(8) Å) is slightly longer than that in free ligand. The change in bond length is also reflected as absorption shift in IR spectrum.

3.2.3. *Crystal structure of complex 2*

Fig. 3 shows the crystal structure of complex **2** characterized by X-ray single crystal diffraction. **2** was synthesized using the same ligand and solvent as complex **1** only different in anion (BF_4^-). In one asymmetric unit, only one crystallographically independent Ag(I) center existed and is confined by two N atoms from distinct ligands as well as one S donor from another ligand, displaying a Y-shape trigonal arrangement (N2C-Ag1-N1A = 135.0(5)°, N2C-Ag1-S1 = 114.8(3)°, N1AC-Ag1-S1 = 104.4(3)°).

For ligand, it could coordinate with metal ions via its thienyl S atoms and/or other coordination atoms of functional groups to form diverse coordination structures. However, thienyl S atoms are scarcely involved into coordination sphere in previous dithienylethene-based complexes [38,51]. In this study, the bond length of Ag1-S1 is 2.689(4) Å, which is well within the range of Ag-S distances in Ag-thiophene complexes [52–55]. It represents the first example of Ag ions binding to S donor of dithienylethene based on perfluorocyclopentene. The Ag-N distances in complex **2** is 2.158(12) Å and 2.192(12) Å, respectively, which is significantly shorter than the distance between Ag ions and S donor. In fact, these bonding parameters are inconsistent with conventional expectation that the soft silver metal forms a stronger bond with the softer sulfur atom rather than the harder nitrogen atom.

Complex **2** exhibits a 1D ladder (or double chain) structure with the neighboring ligands arranged in a *syn-anti* fashion. The cyanophenyl planes of ligands in two inter-connected 1D chains are parallel each other and stack in an offset or slipped fashion. The plane – plane distances between two adjacent benzene rings are 3.56 Å and 3.65 Å, respectively. The corresponding centroid-centroid distances (3.98 Å and 4.13 Å) and displacement angle (26.6° and 27.8°) exceed the maximum parameters for π-π interactions (3.8 Å and 20°), indicating no obvious π-π interactions [56].

In complex **2**, the ligand acts as a linker to bind Ag(I) ions. Ligand retains its anti-parallel fashions of two thienyl rings with dihedral angel of 68.24°. The reactive carbon distance for photo-cyclization between C11 and C21 is 3.79 Å, still close for a ring-closure from 1,3,5-hexatriene to cyclohexadiene. The mean torsion angles between thiophene and hexafluorocyclopentene rings (C(13)-C(17)-C(18)-C(19) and C(17)-C(13)-C(10)-C(9)) are 127.48° and 125.81°, respectively. Different from complex **1**, the cyanophenyl and thienyl rings are almost coplanar in **2**, which is similar to free ligand. This feature favors interactions between the metal ion and the diarylethene groups.

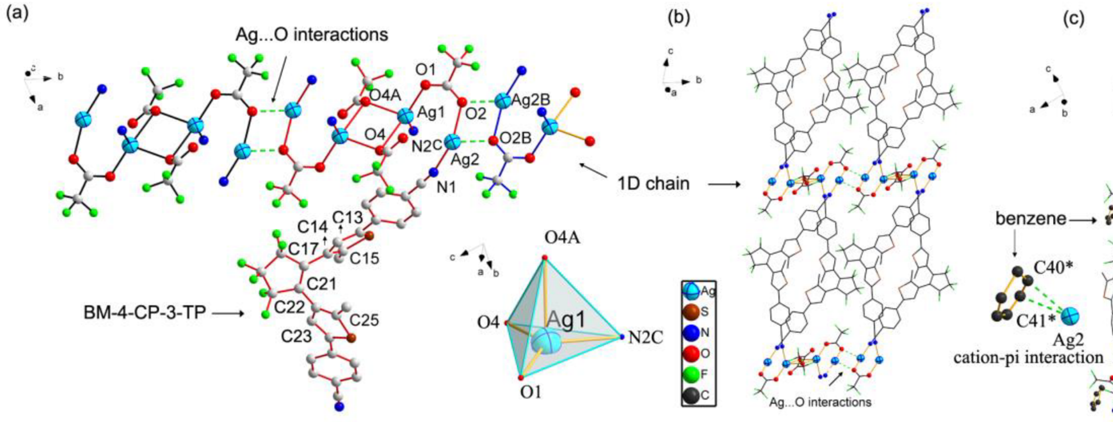

Fig. 2. Crystal structures of complex **1** showing (a) chain structure, (b) Ag…O interactions and (c) cation-π interactions between Ag ion and guest benzene. H atoms are omitted for clarity. Symmetry code:A:1-x,2-y,2-z; B:1-x,3-y,2-z;C:2-x,2-y,1-z.

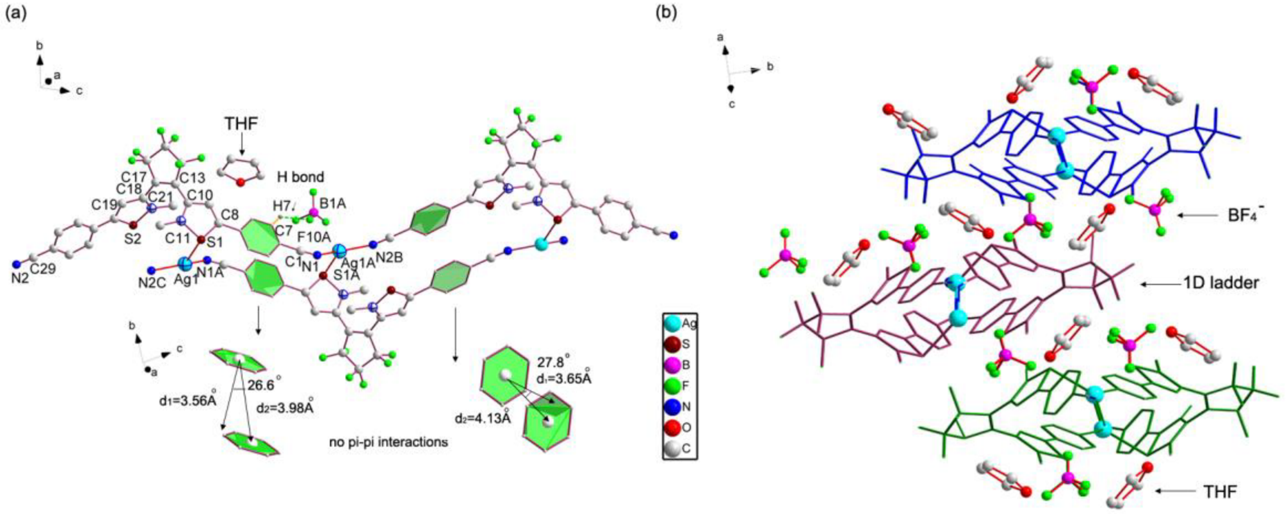

Fig. 3. Crystal structures of complex **2** showing (a) coordination structure, (b) 1-D ladder. Only the H atoms involved in H bond are displayed. Symmetry code:A:1-x,2-y,2-z; B:1-x,3-y,2-z;C:2-x,2-y,1-z.

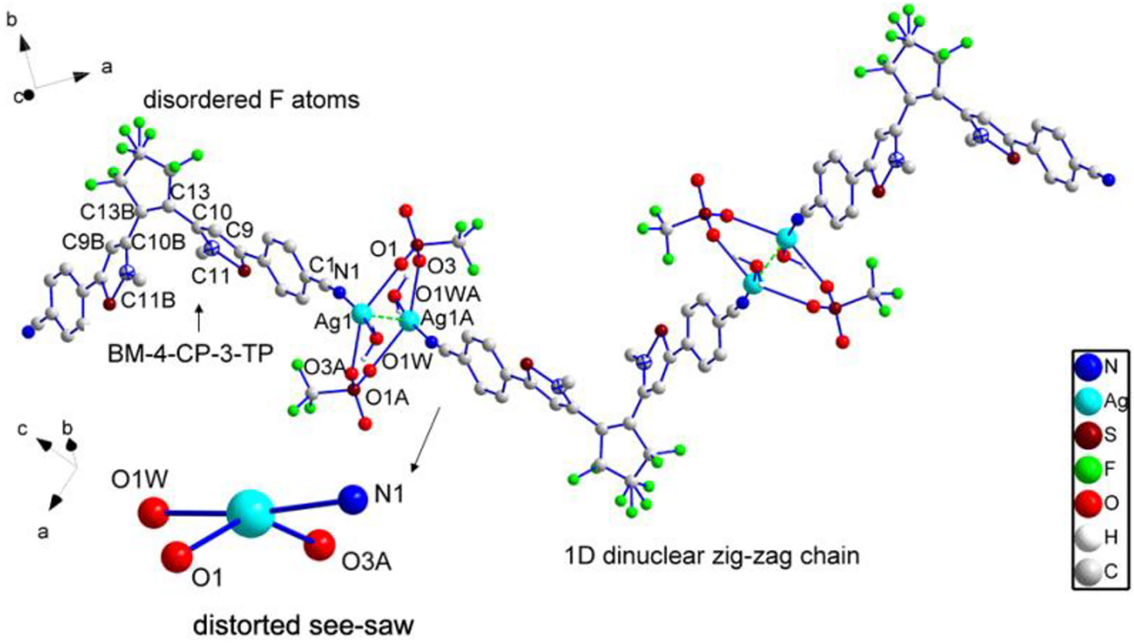

Fig. 4. Crystal structure of complex **3**. Only the H atoms involved in coordination are displayed for clarity. Symmetry code: A: 0.5-x,0.5-y,1-z; B:-x,y,-0.5-z;

Table 2
Summary of ligand and complexes **1–3**.

	ligand	1	2	3
anions		CF_3COO^-	BF_4^-	$CF_3SO_3^-$
dihedral angle A (°)	6.75	40.07	3.48/12.49	22.22
dihedral angle B (°)	51.26	49.28 51.78	59.72 55.77	45.73
Reactive C distance (Å)	3.65	3.65	3.79	3.57
coordination atoms		Only N atom	N and S atoms	Only N atom
weak interactions		Ag…O Ag…C Ag…Ag	H bond	Ag…Ag
λ_{max}(closed-form, nm)	607	619	625	623
time to PSS (min)	35	40	30	25

A: dihedral angle between cyanophenyl and thiophene rings. B: dihedral angle between cyclopentene and thiophene rings.

As an un-coordinating anion, BF_4^- is revealed as ionic guests counterbalancing the framework charge. It is sandwiched between two neighboring 1D ladders via weak intramolecular hydrogen bond between the F atoms of anion and H atoms of ligand. THF molecules, using as crystallization solvent, are also contained in complex **1** acting as guest intercalated into the adjacent ladders.

3.2.4. Crystal structure of complex 3

Fig. 4 illustrates the 1D dinuclear zig-zag chain of **3**, with neighboring ligands packed in a *syn-anti* fashion. The crystallographically independent Ag(I) center is four-coordination and adopts a $[AgN_1O_3]$ coordination environment. The τ_4 value of 0.28 suggests a see-saw structure. Two O atoms are from the distinct $CF_3SO_3^-$ (Ag1-O1 = 2.579(12) Å and Ag1-O3A = 2.557(10) Å) and the third O atom belongs to H_2O (Ag1-O1W = 2.200(10) Å).

$CF_3SO_3^-$ is a moderately coordinating anion and only a few reports are engaged in the coordinated CF_3SO_3 [57,58]. The bond distances of

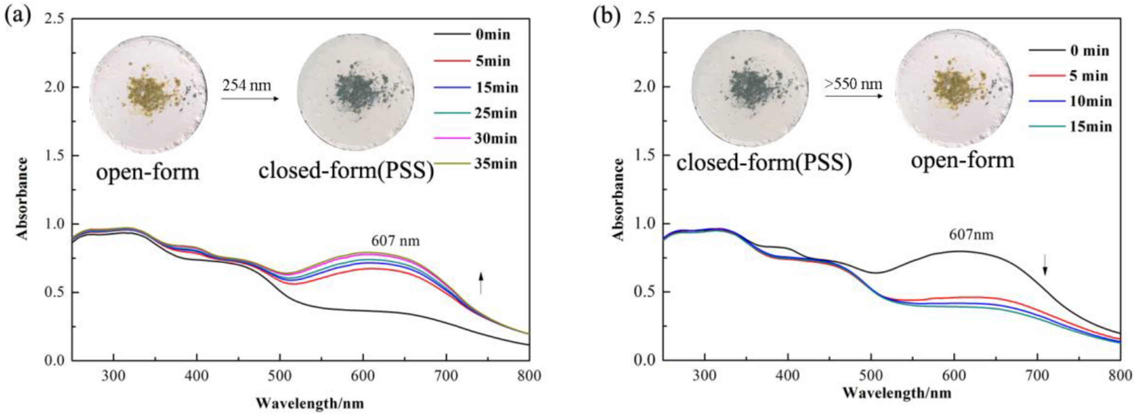

Fig. 5. Time-dependent UV–Vis spectra of BM-4-CP-3-TP in solid state (a) irradiation with 254 nm light and (b) irradiation with ≥550 nm light.

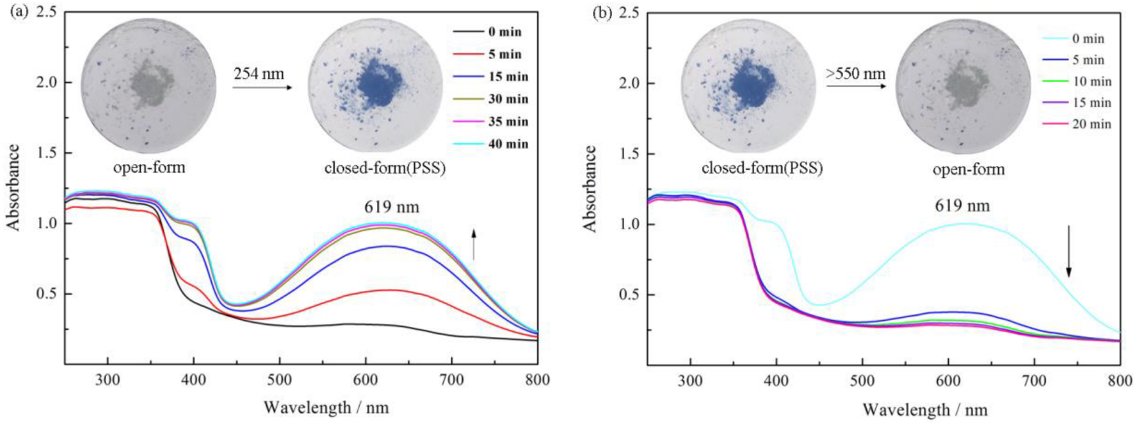

Fig. 6. Time-dependent UV–Vis spectra of complex **1** in solid state (a) irradiation with 254 nm light and (b) irradiation with ≥550 nm light.

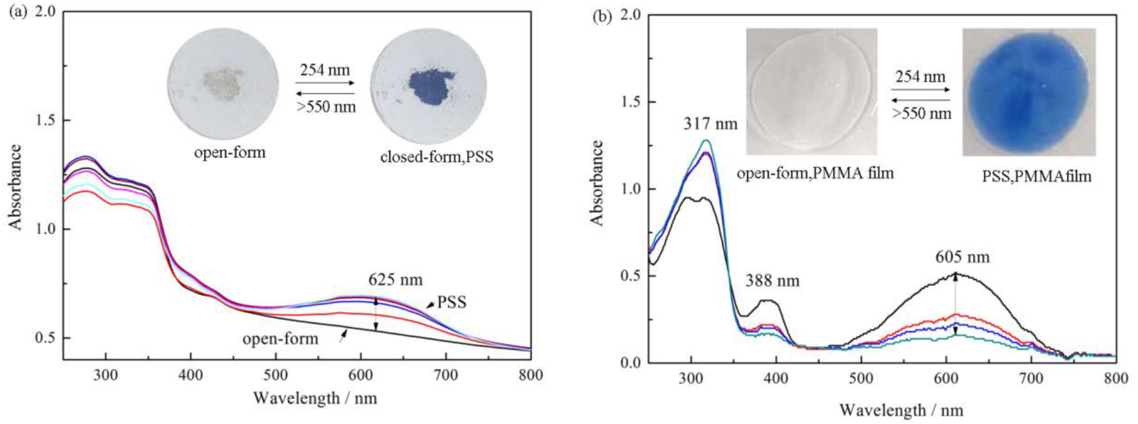

Fig. 7. UV–Vis spectra of **2** in solid state (a) and in PMMA films (b).

Ag-O (anions) in **3** are much longer than those in **1**, demonstrating the weaker coordination ability of $CF_3SO_3^-$ in comparison to CF_3COO^-. In **3**, $CF_3SO_3^-$ shows μ_2-η_1:η_1-bridging mode to link two Ag(I) ions forming an eight-membered dinuclear unit. These dinuclear units are further connected by bridging ligands to yield 1D chain. The distance between two Ag ions is 3.359 Å, which is slightly shorter than the twice van der Waals radius of silver ions (3.44 Å), indicating weak Ag···Ag interaction.

As for ligand, it still retains its anti-parallel arrangement of two thienyl rings with dihedral angel of 58.80° and C···C separation of the photoactive carbon atoms of 3.57 Å. Thus, the structural requirement for photo-cyclization in solid state is fulfilled. The mean torsion angles between thiophene and hexafluorocyclopentene rings (C(13)-C(13B)-C(10B)-C(9B)) is −136.93°. In order to coordinate with Ag(I) ions, ligand rotate its structure with changing considerably the dihedral angle between cyanophenyl and thienyl rings from 6.748° in ligand to 22.22° in complex **3**.

3.2.5. *Anions effect*

During the coordination of ligand with metal ions, ligand conformations are elaborately modulated through non-covalent interactions in three complexes. Anions play an especially un-neglectable role in regulating the configurations of ligands to satisfy the coordination spheres. Complexes **1**–**3** were constructed by same building blocks, metal ions and solvents however anions with different coordination

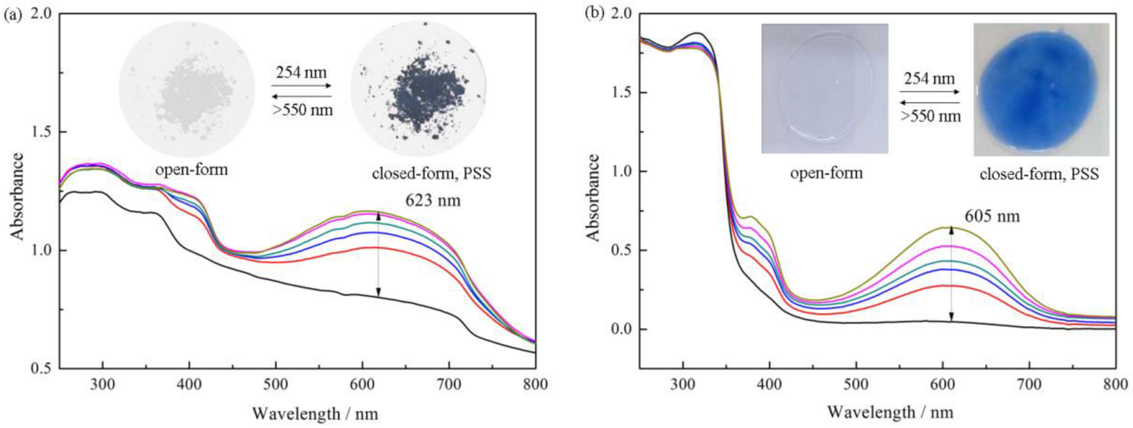

Fig. 8. UV–Vis spectra of **3** in solid state (a) and in PMMA films (b).

abilities. As is expected, three complexes possess different structures. The structural adjustment of ligands in complexes **1**–**3** are mainly reflected in the following two respects:

1) The dihedral angles between cyanophenyl and thiophene rings. The angel is 6.75° in free ligand, and it increase to 40.07° and 22.22° in complexes **1** and **3**, respectively where the anticipated anions is strongly coordinating CF_3COO^- and moderately coordinating $CF_3SO_3^-$, respectively. Whereas in complex **2** using non-coordination BF_4^-, the dihedral angles are 3.48° and 12.49°, which is closer to that in free ligand. Stronger anion promotes bigger changes of dihedral angles between cyanophenyl and thiophene rings of ligand. In complexes, the interactions between metal ions and diarylethene groups are greatly affected by the dihedral angles between cyanophenyl and thiophene rings. So it can be anticipated that the absorption characteristics of the three complexes maybe different due to the anion-directed structural differences.

2) The dihedral angles between cyclopentene and thiophene rings. The angles of complexes **1**–**3** also change in varying degrees in comparison with the corresponding value in ligand. The angle is 51.26° in ligand and changed to 49.28° and 51.78° in complex **1**, 59.72° and 55.77° in complex **2** and 45.73° in complex **3**, respectively. This angle plays a crucial role in the reactive carbons distance. The value of the angle in complex **3** is the smallest one of the three and accordingly complex **3** has the shortest reactive carbon distance (Table 2). And complex **2** possess the biggest dihedral angle and the longest separation of reactive carbons. In addition, in complex **2**, anion doesn't take part in coordination whereas the thiophene group of ligand is found to coordinate with metal ions through S atoms. This coordination feature may also contribute to the longer reactive carbon distance in complex **2**.

*3.3. Photochromism of BM-4-CP-3-TP and complexes **1**–**3** in solid state*

The photochromism of BM-4-CP-3-TP in hexane and thin film were reported previously [40]. The maximum absorption of thin films of pure compound deposited onto quartz in PSS is 591 nm. Because dithienylethenes have the unique ability to undergo reversible photo-switching in solid phase and X-ray diffraction shows a favorable structure of BM-4-CP-3-TP for solid-state photochromism, i.e., the anti-parallel conformation and the short distance between the reacting carbon atoms, the powder state photochromism of ligand is expected and examined. As presented in Fig. 5, the photo-isomerizations between the open and closed forms of ligand occurred reversibly in solid state with the absorption attributable to closed-ring isomer maintaining at 607 nm. This maximum absorption is different from that of previous report (591 nm), indicating that the solid structure of BM-4-CP-3-TP investigated herein is different from that of deposited onto quartz in literature. It takes 35 min of photo-irradiation for ligand to achieve the PSS and 15 min for photo-reversion in solid state.

Although there are H bonds and π-π interactions in complexes **1**–**3**, our previous results showed that these weak non-covalent interactions have a non-significant effect on ring-closure due to their minor suppression to the rotation of thiophene rings [27,35]. Therefore, photo-switching of three metal complexes are further investigated in solid state.

UV–vis absorption spectra for complexes **1**–**3** are illustrated in Figs. 6–8. As anticipation, the photo-switching of the ligand in these complexes is effective. Irradiating the three powdered complexes with UV light (254 nm) resulted in appearances of broad absorption bands in the visible region corresponding to ring-closed isomer with color changed from colorless to blue, indicating the successful forward photo-reactions (ring-closing). Exposing the colored complexes to visible light (> 550 nm) drove the reverse backward photo-reactions (ring-opening) and regenerated both the original color and the absorption spectra.

In the photo-cyclization, chemical bond rearrangement requires the rotation of thiophene rings to form a new bond. However, this change in orientation and volume from the rotation might cause perturbation upon others due to ligand being packed in rigid and infinite frameworks. Less favorable, the cyanophenyl of ligand participates in not only coordination bonds but also intermolecular H bonds, which may further restrict the free rotation of thiophene rings. Even so, all three complexes displayed reversible and effective photochromism in solid phase, indicating a cooperative effect of elastic coordinative behavior of metal ions [59].

Similarities in spectral and color changes of the three complexes were observed upon comparison with the characteristics of the corresponding metal-free ligand (λ_{max} = 607 nm). Three complexes in PSS showed red-shifts of maximum absorption bands of 12 nm, 18 nm and 16 nm, respectively, indicating a pronounced coordination effect (λ_{max} is 619 nm, 625 nm and 623 nm for complexes **1**–**3**, respectively). In addition, much faster conversion rates for complexes **2** and **3** in solid phase were observed as compared to free ligand (the irradiation time to achieve the PSS is 35 min for ligand, Table 2). Therefore, metal coordination doesn't prohibit the photo-responsive performance of ligand but exerts an advantageous effect on the regulation of optical properties.

Because thin films based on polymers can be used to tune a wide range of surface properties, which is beneficial to the practical applications in storage memory, all complexes were further shaped into PMMA films. These films all exhibit expected reversible photochromism triggered by alterative irradiation with UV light and visible light (Fig. 7(b), 8(b) and S5), indicating their promising potential for future applications.

3.4. Discussions of structure-property relationship

Although all complexes displayed efficient photochromism in solid state indicating metal coordination doesn't suppress both ring-closure and ring-opening, there are some differences in their absorptions of worthy discussing.

Firstly, the maximum absorptions of three complexes in closed-form

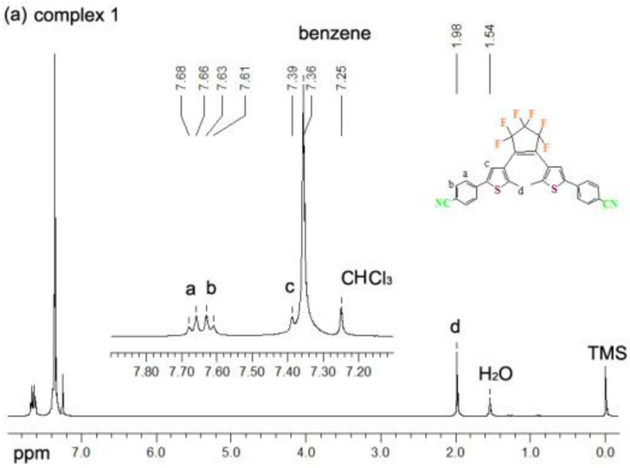

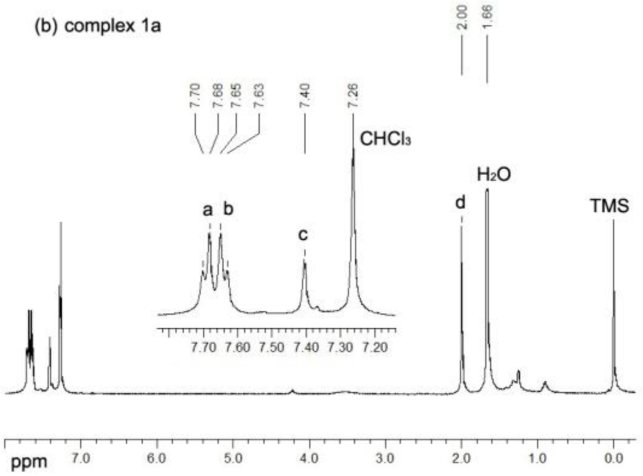

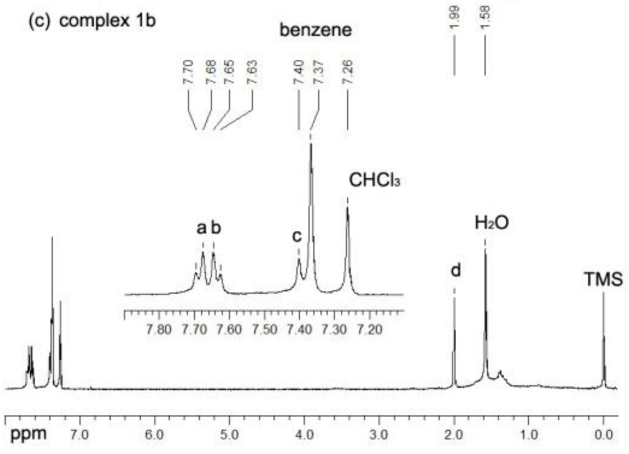

Fig. 9. ^{1}H NMR spectra of **1** and its derivatives in $CDCl_3$ at room temperature: (a) **1**, (b) **1a**, and (c) **1b**.

are different. Complex **2** present the longest absorption at 625 nm followed by complex **3** at 623 nm and complex **1** at 619 nm (Table 2). This phenomenon can be explained by the structural distinctions of the three complexes. As described previously, the interactions between metal ions and ligands are greatly affected by the dihedral angles between cyanophenyl and thiophene rings. A smaller dihedral angle will facilitate the metal–ligand interactions and exert a more signally influence on the photochromism. Complex **2** has the smallest dihedral angle and thus the strongest electronic delocalization. In experimental, it illustrate consistently the most significantly red-shifts in absorption (18 nm). Besides, complex **2** has the biggest dihedral angle change (*c.a.* 8°, Table 2) between cyclopentene and thiophene rings related to the free ligand (6° for **3** and 2° for **1**, respectively). This dissimilarity as ligand is also responsible for its as much as 18 nm red-shifts in absorption.

Secondly, the time to reach PSS is varied in three complexes. This may closely related to the interactions existed in complexes because the non-covalent bonds, such as metal-coordinating bonds, hydrogen bonds, Van de Waals contacts and aromatic-aromatic interactions are considered to have a role in the photo-induced isomerizations when dithienylethenes are self-assembled into coordination networks. As shown in Table 2, there are Ag···O interactions, Ag···π interactions and weak Ag···Ag interactions except coordinating bonds in complex **1** whereas only either hydrogen bonds or Ag···Ag interactions exist in complex **2** and **3**. So, complex **1** has the most complicated interactions among three complexes, which led to comparably the greatest suppression of photo-cyclization and the longest time to reach PSS (40 min). In complex **2**, besides N atoms, S atoms are also involved in coordination, which resulted in a longer time to PSS (30 min) than that for complex **3** (25 min).

Therefore, incorporation of metal ions into photochromic building blocks, especially selection of anions with different coordinating abilities, is a smart strategy to regulate the photophysical and photochemical properties on the premise of retaining the reversible photochromism. The absorption properties of complexes can be regulated finely by varying merely the type of anions.

*3.5. Guest desorption-readsorption properties of complex **1***

Complex **1** is revealed as a guest-incorporated structure and thus its guest desorption-readsorption properties were further investigated. It's known that the reversible structure transformation between two isomers of dithienylethenes during photo-isomerizations will cause a volume change. It will shrink in photo-cyclization with open-isomer transferred to closed-isomer and expand in photo-reversion with closed-isomer returned to original open-isomer. Previous studies showed diarylethenes were incorporated into MOFs to affect the porosity and then gas sorption properties [24,60] as well as anions uptake and release triggered by light [61]. However, whether the photo-induced volume change of the framework **1** originating from ligand shrinkage could lead to desorption of guests still remains great challenge, since the geometry of solvent is much larger than the reported gas molecules and ions.

Unfortunately, our attempts to liberate the guests by light-stimulus are not successful. ^{1}HNMR examination results showed that after photo-irradiation of complex **1** with UV light, the benzene signals didn't disappear or weaken in the ^{1}HNMR spectrum, suggesting unsuccessful guest-desorption by light excitation. This observation indicated that the conformational change of framework during the photo-reaction is not sufficiently enough to induce the liberation of guest in the present system. In this work, single crystals of complex **1** are not stable enough to keep their crystallinity after photo-cyclization. So the exact volume change of complex **1** is unavailable. According to the previous reported single-crystal to single-crystal photo-cyclization, the volume change of ligand is as small as 3 Å^{3} [62]. During light irradiation, the shrinkage of ligand driven by the photo-cylization will lead to the corresponding shrinkage of the 2D layers in complex **1** (Fig. S6). However, this shrinkage of 2D layers occurs in the *bc* plane and may has a little impact on the spaces between two neighboring layers where the guests are nested. In other words, the spaces for accommodation of the guests didn't change significantly. In addition, the cation-π interactions between guest benzene and host framework may have an extra disadvantageous role in the photo-responsive guest desorption.

But for all this, it offers a possible strategy to allow the photo-triggered guest release which is however generally realized by heating or pressure, and our related researches will be addressed in later program.

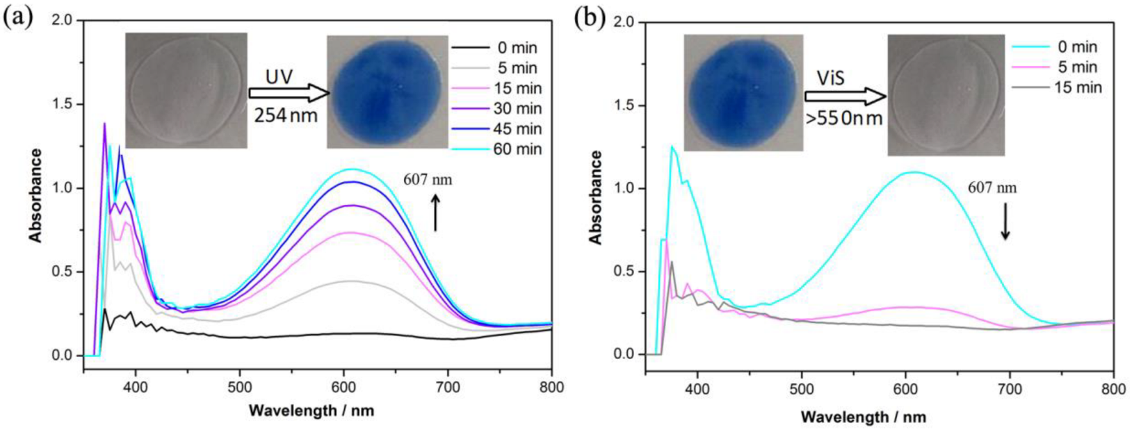

Fig. 10. Time-dependent UV–Vis spectra of complex **1a** in solid films (a) irradiation with 254 nm light and (b) irradiation with ≥550 nm light.

3.5.1. *Elimination of guests by heating*

The elimination of guest for **1** was then performed by heating. According to thermogravimetric (TG) analysis**,** a weight loss corresponding to the liberation of two mol benzene molecules (13.25%, calcd.13.37%) occurred below 80 °C (Fig. S7) and the second weight loss of 19.11% is assigned to the anions (calcd.19.34%). ^{1}HNMR analysis was used to provide the additional evidence of the complete release of guests. As shown in Fig. 9a, the chemical shift at 8.05 ppm is assigned to the H signals of phenyl of ligand and the ^{1}HNMR resonance observed at 7.35 ppm indicated the presence of benzene in **1**. Whereas, the ^{1}HNMR resonances attributed to benzene vanished completely after heating, supporting the thorough elimination of benzene in **1** (Fig. 9b). Therefore, guest-free **1a** could be obtained by heating of **1** under monitoring with TG analyzer.

The structure of **1a** was further examined. Due to the loss of crystallinity XRPD of complexes **1** and **1a** are not successful. Our previous study showed that IR can provide useful information of structural changes, e.g. the exact coordination modes of COO^- [34]. The IR spectrum of **1a** was then measured whereas the vibration peaks assigned to CF_3COO^- remains almost unchanged indicating the anion keep its coordination mode upon the elimination of guest molecule (Fig. S8).

3.5.2. *Reincorporation of guests*

Exposing the de-solvated **1a** to benzene vapor yielded **1b.** As shown in Fig. 9c, the ^{1}HNMR resonance of benzene (7.35 ppm) was witnessed again in **1b**, and the estimated ratio of re-adsorpted benzene is *c.a.* 55.2% based on integration approach. These evidences suggested that the guest molecules in **1** can be removed by heating and included again by absorption.

Toluene was further selected as new target for absorption due to its similar chemical structure as benzene yet slightly larger geometry. However, no resonance signals attributed to toluene was observed in the ^{1}HNMR spectrum of **1c** (Fig. S9), suggesting the declined accommodation of toluene in **1a**. As a conclusion, the solvated benzene in **1** can be released, reincorporated but not replaced by toluene.

3.5.3. *Photochromism of the guest-desorbed **1a***

The photo-isomerization of **1a** was investigated in solid films. Fig. 10 illustrated the UV spectra of **1a** and, interestingly, it showed reversible spectral changes with color transformation between colorless and blue. The maximum absorption at 607 nm of PSS is as same as that of **1**. This observation indicates that the dithienylethene backbone in **1a** didn't collapse after guest liberation. Our previous example showed the maintained photochromism upon heating to lose of the coordinated solvent [34]. Herein, the present result exhibits the other effective sustainability of photochromism after the release of guest.

4. Conclusions

A cyano-functionalized dithienylethene was synthesized and employed as photo-responsive receptor to construct three new hybrid systems by incorporation of Ag (I) salts. The key design aspect is to tailor the photo-induced absorption properties of the resulted complexes by selecting anions with different coordinating abilities to collaborate with the metal ions and organic component. The three complexes derived from different anions exhibit expectedly distinct coordination structures, ligand configuration and non-covalent interactions. The Ag(I) coordination induces some perturbation of the photochromic behavior, especially, anions enable successfully the fine tuning of the absorptions of ligand. The present study thus demonstrates that combining inorganic metal salts with organic photochromic compound to form hybrid materials by metal coordination and judicious anions selection at molecular level could realize the convenient regulation of reversible photo-responsive isomerizations. The finding will contribute to design and elegant modulation of photochromic compounds through crystal engineering based approach.

CRediT authorship contribution statement

Jing Han: Conceptualization, Funding acquisition, Methodology, Software. Writing - original draft, Writing - review & editing. **Qing Li:** Investigation. **Zhong Yu:** Conceptualization, Supervision, Funding acquisition. **Chun-yan Quan:** Investigation. **Xiang Liu:** Investigation. **Jia-cai Han:** Investigation.

Declaration of Competing Interest

The authors declare that they have no known competing financial interests or personal relationships that could have appeared to influence the work reported in this paper.

Acknowledgments

This work is supported by a grant for Scientific Research Foundation for the Returned Overseas Chinese Scholars, State Education Ministry (Yu Zhong), Natural Science Foundation of China (No 51679190), Shaanxi Provincial key research and development Projects (Nos 2018PT-27, 2018 GY-125 and 2019 NY-201) and China Scholarship Council (CSC201808615022).

Appendix A. Supplementary data

Details about additional structure graphics, IR, ^{1}HNMR, and TGA. Crystallographic data for the structure in this paper has been deposited with the Cambridge Crystallographic Data Centre, CCDC, 12 Union Road, Cambridge CB21EZ, UK. Copies of the data can be obtained free of charge on quoting the depository number CCDC 1953339, 1953341, 1953342, 1953343 (E-Mail: deposit@ccdc.cam.ac.uk, http://www.ccdc.cam.ac.uk). Supplementary data to this article can be found online at https://doi.org/10.1016/j.ica.2020.119666.

References

[1] M. Irie, T. Fukaminato, K. Matsuda, S. Kobatake, Chem. Rev. 114 (2014) 12174.
[2] H. Tian, S. Wang, Chem. Commun. 8 (2007) 781.
[3] G.M. Tsivgoulis, J.-M. Lehn, Adv. Mater. 9 (1997) 627.
[4] K. Matsuda, M. Irie, Chem. Lett. 35 (2006) 1204.
[5] V. Lemieux, S. Gauthier, N.R. Branda, Angew. Chem. 118 (2006) 6974.
[6] Z.Y. Sun, H. Li, G. Liu, C.B. Fan, S. Pu, Z. Dyes Pigments 106 (2014) 94.
[7] J.J. Zhang, H. Tian, Adv. Optical Mater. 6 (2018) 1701278.
[8] C.C. Ko, W.-M. Kwok, W.-W. Vivian, D.L. YamPhillips, Chem. Eur. J. 12 (2006) 5840.
[9] T. Nakagawa, Y. Hasegawa, T. Kawai, Chem. Commun. 37 (2009) 5630.
[10] Y. Lin, J. Yin, J.J. Yuan, M. Hu, Z.Y. Li, G.A. Yu, S.H. Liu, Organometallics 29 (2010) 2808.
[11] T.Q. Wu, N.R. Branda, Chem. Commun. 52 (2016) 8636.
[12] C.-J. Carling, J.-C. Boyer, N.R. Branda, J. Am. Chem. Soc. 131 (2009) 10838.
[13] Z.G. Zhou, H. Hu, H. Yang, T. Yi, K.W. Huang, M.X. Yu, Chem. Commun. 39 (2008) 4786.
[14] J.H. Liang, J. Yin, Z.Y. Li, C. Zhang, D. Wu, S.H. Liu, Dyes Pigments 91 (2011) 364.
[15] M. Milek, F.W. Heinemann, M.M. Khusniyarov, Inorg. Chem. 52 (2013) 11585.
[16] M. Nihei, Y. Suzuki, N. Kimura, Y. Kera, H. Oshio, Chem. Eur. J. 19 (2013) 6946.
[17] B. Rösner, M. Milek, A. Witt, B. Gobaut, P. Torelli, R.H. Fink, M.M. Khusniyarov, Angew. Chem. Int. Ed. 54 (2015) 12976.
[18] T. Shiga, H. Miyasaka, Yamashita, M. Morimoto, M. Irie, Dalton Trans. 40 (2011) 2275.
[19] L. Ordronneau, V. Aubert, V. Guerchais, A. Boucekkine, H. Le. Bozec, A. Singh, I. Ledoux, D. Jacquemin, Chem. Eur. J. 19 (2013) 5845.
[20] V. Aubert, V. Guerchais, E. Ishow, K. Hoang-Thi, I. Ledoux, K. Nakatani, H. Le. Bozec, Angew. Chem. Int. Ed. 47 (2008) 577.
[21] D.K. Cao, R.H. Wei, X.X. Li, Y.W. Gu, Dalton Trans. 44 (2015) 5755.
[22] D.K. Cao, J.Q. Feng, M. Ren, Y.W. Gu, Y. Song, M.D. Ward, Chem. Commun. 49 (2013) 8863.
[23] V. Guerchais, L. Ordronneau, H. Le. Bozec, Coord. Chem. Rev. 254 (2010) 2533.
[24] F. Luo, C.B. Fan, M.B. Luo, X.L. Wu, Y. Zhu, S.Z. Pu, W.Y. Xu, G.C. Guo, Angew. Chem. Int. Ed. 53 (2014) 9298.
[25] W.J. Tan, J. Zhou, F.Y. Li, T. Yi, H. Tian, Chem. Asian J. 6 (2011) 1263.
[26] D.K. Cao, R.H. Wei, X.X. Li, J.F. Chen, M.D. Ward, Dalton Trans. 44 (2015) 4289.
[27] J. Han, S. Li, Z. Yu, H. Chen, Y. Zang, Q.J. Wang, Inorg. Chim. Acta. 464 (2017) 11.
[28] J. Thomas, D. Kumar, A. Ramanan, Inorg. Chim. Acta 96 (2013) 126.
[29] S. Hazra, L.M. Martins, M.F.C.G. da Silva, A.J.L. Pombeiro, Inorg. Chim. Acta 455 (2017) 549.
[30] S.M. Zhang, Y.H. Chen, L.H. Wang, G.X. Wang, J. Solid State Chem. 226 (2015) 201.
[31] S.C. Chen, R.R. Qin, Z.H. Zhang, J. Qin, H.B. Gao, F.A. Sun, M.Y. He, Q. Chen, Inorg. Chim. Acta 390 (2012) 61.
[32] M. Munakata, J. Han, A. Nabei, T. Kuroda-Sowa, M. Maekawa, Y. Suenaga, N. Gunjima, Polyhedron. 25 (20006) 3519.
[33] M. Munakata, J. Han, A. Nabei, T. Kuroda-Sowa, M. Maekawa, Y. Suenaga, N. Gunjima, Inorg. Chim. Acta 359 (2006) 4281.
[34] J. Han, M. Maekawa, Y. Suenaga, H. Ebisu, A. Nabei, T. Kuroda-Sowa, M. Munakata, Inorg. Chem. 46 (2007) 3313.
[35] J. Han, H. Chen, Z. Yu, P. Guo, Inorg. Chim. Acta 462 (2017) 1.
[36] J. Han, J.C. Han, Z. Yu, Y. Zang, B. Jin, Chin. J. Struct. Chem. 37 (2018) 1663.
[37] M. Munakata, J. Han, M. Maekawa, Y. Suenaga, T. Kuroda-Sowa, A. Nabei, H. Ebisu, Inorg. Chim. Acta. 360 (2007) 2792.
[38] J. Han, H. Konaka, T. Kuroda-Sowa, M. Maekawa, Y. Suenaga, H. Isihara, M. Munakata, Inorg. Chim. Acta 359 (2006) 99.
[39] G. Liu, Q.D. Tu, Q. Zhang, C.B. Fan, T.S. Yang, Acta Cryst. E64 (2008) o938.
[40] R. Castagna, V. Nardone, G. Pariani, A. Biancoc, J. Photochem. Photobiol. A: Chem. 325 (2016) 45.
[41] D.T. Cromer, J.T. Waer, International Tables for X-ray Crystallography; The Kynoch Press: Birmingham, England, 1974; Vol IV.
[42] Crystal Structure Analysis Package; Rigaku/MSC, Inc.: Woodlands, TX, 1985 and 1992.
[43] G.M. Sheldrick, SHELXS-97, Program for the Solution of Crystal Structures, University of Gottingen, Göttingen, Germany, 1997.
[44] J.L. Fillaut, N.N. Dua, F. Geneste, L. Toupet, S. Sinbandhit, J. Organomet. Chem. 691 (2006) 5610.
[45] R.L. Cordiner, D. Albesa-Jove, R.L. Roberts, J.D. Farmer, H. Puschmann, D. Corcoran, A.E. Goeta, J.A.K. Howard, P.J. Low, J. Organomet. Chem. 690 (2005) 4908.
[46] M.L. Kuznetsov, A.J.L. Pombeiro, Dalton Trans. 3 (2003) 738.
[47] M.L. Kuznetsov, E.A. Klestova-Nadeeva, A.I. Dement'ev, J. Mol. Struct. –Theochem. 671 (2004) 229.
[48] M.L. Kuznetsov, J. Mol. Struct.–Theochem. 674 (2004) 33.
[49] V.T. Yilmaz, E. Senel, E. Guney, C. Kazak, Inorg. Chem. Commun. 11 (2008) 1330.
[50] M. Munakata, L.P. Wu, G.L. Ning, Coord. Chem. Rev. 198 (2000) 171.
[51] H. Konaka, L.P. Wu, M. Munakata, T. Kuroda-Sowa, M. Maekawa, Y. Suenaga, Inorg. Chem. 42 (2003) 1928.
[52] G.C. Van Stein, G. Van Koten, F. Blank, L.C. Taylor, K. Vrieze, Inorg. Chim. Acta 98 (1985) 107.
[53] Y.B. Dong, Y. Geng, J.P. Ma, R.Q. Huang, Organometallics 25 (2006) 447.
[54] E.C. Constable, C.E. Housecroft, P. Kopecky, M. Neuburger, J.A. Zampese, Inorg. Chem. Commun. 27 (2013) 159.
[55] H.K. Lee, S.W. Lee, Bull. Korean Chem. Soc. 28 (2007) 421.
[56] C. Janiak, J. Chem. Soc. Dalton Trans. 21 (2000) 3885.
[57] F. Hung-Low, K.K. Klausmeyer, Inorg. Chim. Acta 361 (2008) 1298.
[58] K.V. Kilway, S. Deng, S. Bowser, J. Mudd, L. Washington, D.M. Ho, Pure Appl. Chem. l78 (2006) 855.
[59] M. Munakata, L.P. Wu, J. Am. Chem. Soc. 118 (1996) 3305.
[60] Y.T. Zheng, H. Sato, P.Y. Wu, H.J. Jeon, R. Matsuda, S. Kitagawa, Nature Commun. 8 (2017) 100.
[61] M.X. Han, R. Michel, B. He, Y.S. Chen, D. Stalke, M. John, G.H. Clever, Angew. Chem. Int. Ed. 52 (2013) 1319.
[62] T. Yamada, S. Kobatake, M. Irie, Bull. Chem. Soc. Jpn. 73 (2000) 2179.